Frontiers in Bioscience Landmark

Front. Biosci. (Landmark Ed) **2026**; 31(8): 53140
https://doi.org/10.31083/FBL53140

Original Research

Membrane Potential Hyperpolarization Controls the Osteogenic Differentiation of Human Dental Follicle Stem Cells by Increasing Intracellular Ca^{2+} Levels

Yidan Yang[1,2,†], Weijia Du[1,2,†], Dan Yang[1,2], Yuyang Luo[1,2], Qian Zhou[1,2], Dongchuan Zuo[3], Jin Zeng[1,2,*]

[1]Department of Orthodontics, The Affiliated Stomatology Hospital, Southwest Medical University, 646000 Luzhou, Sichuan, China
[2]Luzhou Key Laboratory of Oral & Maxillofacial Reconstruction and Regeneration, The Affiliated Stomatology Hospital, Southwest Medical University, 646000 Luzhou, Sichuan, China
[3]Key Laboratory of Medical Electrophysiology, Ministry of Education & Medical Electrophysiological Key Laboratory of Sichuan Province, Institute of Cardiovascular Research, Southwest Medical University, 646000 Luzhou, Sichuan, China
*Correspondence: zengjin@swmu.edu.cn (Jin Zeng)
[†]These authors contributed equally.
Academic Editor: Francesca Diomede
Submitted: 21 April 2026 Revised: 26 June 2026 Accepted: 30 June 2026 Published: 18 August 2026

Abstract

Background: Kir2.1 channels are responsible for membrane hyperpolarization of many cell types. While these Kir2.1 channels are known to be necessary for proper bone development and play a critical role in osteogenesis, the underlying mechanisms remain poorly understood. Here, we examined the effect of Kir2.1-mediated membrane hyperpolarization on the osteogenic differentiation of human dental follicle stem cells (hDFCs), a type of mesenchymal stem cell (MSC), and explored the underlying mechanisms. **Methods:** Levels of Kir2.1 and osteogenic marker expression were evaluated by quantitative real-time polymerase chain reaction (qRT-PCR) and western blotting. Alkaline phosphatase (ALP) and Alizarin red staining were employed to evaluate ALP enzymatic activity and mineralized nodule formation, respectively. Intracellular Ca^{2+} levels were measured using fluorescent Ca^{2+} indicators with Ca^{2+} imaging. **Results:** Reversal of membrane hyperpolarization via modulation of extracellular K^+ concentration ($[K^+]_e$) was shown to suppress osteogenic differentiation of hDFCs, whereas the induction of membrane hyperpolarization through the opening of ATP-sensitive K^+ channels had the opposite effect, enhancing hDFC osteogenesis. Kir2.1 channel expression was upregulated during the osteogenic differentiation of hDFCs. Inhibition of Kir2.1 using short hairpin RNA (shRNA) or a pharmacological inhibitor suppressed osteogenic differentiation. Hyperpolarizing the membrane by decreasing $[K^+]_e$ led to the elevation of intracellular Ca^{2+} levels, whereas this effect was eliminated by the removal of extracellular Ca^{2+}, Kir2.1 inhibition, or treatment with La^{3+}, a store-operated Ca^{2+} channel (SOC) blocker. **Conclusions:** Our findings indicate that membrane hyperpolarization promotes osteogenic differentiation of hDFCs by increasing intracellular Ca^{2+} levels and that the Kir2.1 and SOC channels play important roles in this process.

Keywords: mesenchymal stem cells; osteogenesis; membrane potentials; potassium channels

1. Introduction

While stem cell transplantation holds immense promise for tissue regeneration and disease treatment, insights into the fundamental processes controlling stem cell biological behaviors are crucial. Dental follicle cells (DFCs) are dental-derived mesenchymal stem cells (MSCs) capable of differentiating into periodontal ligament cells, cementoblasts, and osteoblasts [1]. In recent years, there has been growing interest in DFCs owing to both their crucial role in tooth eruption and bone remodeling, as well as their potential use for cell-based tissue engineering and disease treatment applications [2].

Kir2.1 channels, encoded by potassium inwardly rectifying channel subfamily J member 2 (*KCNJ2*), are responsible for the membrane hyperpolarization of excitable cells, such as cardiomyocytes and neurons [3]. Increasing evidence has shown that Kir2.1 channels also play an important role in non-excitable cells. For example, the Kir2.1-mediated modulation of macrophage membrane potential serves as a critical regulator of nutrient uptake and downstream metabolic reprogramming, thereby modulating inflammatory responses [4]. Blockade of Kir2.1 channels causes membrane depolarization and thereby enhances endothelial progenitor cell differentiation [5]. Andersen's syndrome is a rare clinical entity defined by the symptomatic triad of periodic paralysis, cardiac arrhythmia, and bone developmental defects [6,7]. In induced pluripotent stem cell MSCs from patients with Andersen's syndrome, loss of Kir2.1 channel function caused by *KCNJ2* gene mutations has been found to impair the osteoblastic process, suggesting a critical role of the Kir2.1 channel during the process of osteogenesis [8,9]. However, the underlying electrophysiological mechanisms have not been investigated at length.

Copyright: © 2026 The Author(s). Published by IMR Press.
This is an open access article under the CC BY 4.0 license.

Publisher's Note: IMR Press stays neutral with regard to jurisdictional claims in published maps and institutional affiliations.

The regulation of Ca^{2+} dynamics plays a central role in MSC differentiation, with Ca^{2+} entry across the plasma membrane representing a key mechanism through which MSCs mobilize their Ca^{2+} stores [10,11]. Electrical stimulation that facilitates Ca^{2+} entry across the plasma membrane enhances the osteogenic differentiation of MSCs [12]. Of the Ca^{2+}-permeable channels expressed in MSCs, store-operated Ca^{2+} channels (SOCs) have been proposed as the main mediators of Ca^{2+} entry through the plasma membrane [10,11,13]. Ca^{2+} influx is driven by the establishment of a Ca^{2+} concentration gradient across the plasma membrane, which is controlled by membrane potential. Membrane hyperpolarization increases the driving force for Ca^{2+} influx, whereas membrane depolarization has the opposite effect [14,15]. Changes in membrane potential can therefore modulate intracellular Ca^{2+} signaling activity by modulating the degree of plasma membrane ion channel Ca^{2+} permeability.

In this study, we investigated the role of Kir2.1-linked membrane hyperpolarization in the differentiation of human DFCs (hDFCs). To gain insight into the functional role of Kir2.1 in these cells, lentiviral vectors were used to stably knock down this protein, after which the osteogenic differentiation capacity of these cells was assessed. Single-cell Ca^{2+} imaging was then performed to examine the effects of Kir2.1-linked membrane hyperpolarization on intracellular Ca^{2+} levels and to identify the pathways of Ca^{2+} entry associated with these effects in hDFCs.

2. Materials and Methods

2.1 Cell Culture and Lentiviral Transduction

Dental follicles were obtained from embedded third molars collected from the orthodontics department at the Affiliated Stomatology Hospital of Southwest Medical University in Luzhou, China. Ethical approval for all human cell culture experiments was obtained from the Ethics Committee of the Affiliated Stomatology Hospital of Southwest Medical University (reference number: 220815003). Primary hDFCs were derived from dental follicle tissues using a previously reported approach [16]. The primary hDFC cell was validated by short tandem repeat (STR) profiling and tested negative for mycoplasma. Briefly, tissue blocks were cut into small pieces and digested with 1% collagenase and 1% dispase at 37°C for 40 min. Dissociated cells and partially digested tissue were then transferred into DMEM (Gibco, Grand Island, NY, USA) containing 10% FBS, 100 U/mL penicillin, and 100 µg/mL streptomycin, followed by culture at 37 °C under 5% CO_2. The culture medium was replaced every 2 days prior to passaging, and all experiments were performed with cells from passages 2–3.

For knockdown experiments, recombinant lentiviral vectors were generated by cloning Kir2.1-specific short hairpin RNA (shRNA) sequences (GCAGATCTGCTAGCGTATATTCTCGAG) or a scrambled non-targeting shRNA into the LV-U6-mPGK-EGFP-T2A-Puro plasmid (Cyagen, Guangzhou, China). In this construct, GFP functions as a reporter for successful transduction. hDFCs were infected with lentiviruses at a concentration of 10^{10} plaque-forming units/mL. Transduced cells were identified based on GFP positivity.

2.2 Osteogenic Differentiation

Osteogenic differentiation was induced by culturing hDFCs in DMEM supplemented with 10% FBS, 10 mM β-glycerophosphate, 10^{-8} M dexamethasone, 50 µg/mL ascorbic acid, and 10 nM vitamin D_3. After 14 days, cells were fixed with 4% paraformaldehyde and subjected to Alizarin red staining to visualize calcium deposits. To quantify the results of this staining approach, the stain was then dissolved in 10% cetylpyridinium chloride monohydrate for 30 min, and absorbance at 562 nm was subsequently read on a microplate reader.

2.3 Measurement of Alkaline Phosphatase Activity

For alkaline phosphatase (ALP) staining, the hDFCs were fixed in 4% paraformaldehyde, washed with phosphate-buffered saline (PBS), and stained according to the ALP Staining Kit (C3206, Beyotime Biotechnology, Shanghai, China) in accordance with the manufacturer's instructions. Stained cells were observed and photographed using a phase-contrast microscope. We also measured ALP activity using a commercial ALP kit (P0321S, Beyotime Biotechnology, Shanghai, China). hDFCs were washed with PBS and incubated in 0.5 mL of 0.2% Triton X-100 in distilled water to lyse cells for ALP activity analysis. Samples were analyzed at 405 nm using a microplate reader, and ALP-specific activity was calculated. Quantification was conducted by dividing the absorbance by the protein concentration, as determined by the BCA protein assay (P0009, Beyotime Biotechnology, Shanghai, China).

2.4 Quantitative Real-Time Polymerase Chain Reaction (qRT-PCR)

Total RNA was purified from hDFCs using TRIzol (Thermo Fisher Scientific, Waltham, MA, USA) per the manufacturer's guidelines. cDNA synthesis was subsequently carried out with the PrimeScript™ RT reagent kit (TaKaRa, Tokyo, Japan). qRT-PCR was performed using an Applied Biosystems Prism 7900HT Sequence Detection System (Thermo Fisher Scientific) with a PrimeScript RT-PCR Kit (TaKaRa). Gene expression levels were normalized to glyceraldehyde 3-phosphate dehydrogenase (*GAPDH*), and the mean fold change in gene expression relative to *GAPDH* was calculated using the $2^{-\Delta\Delta Ct}$ method. Specific primers used for the detection of runt-related transcription factor 2 (*RUNX2*), osteocalcin (*OCN*), and *GAPDH* were synthesized by Sangon Biotech (Shanghai, China). Utilized primers were as follows (5′-3′): Kir2.1: forward TCAGAAGAAGACGGTATGAAGTTGGC, reverse GTGGTGAAGATGTCTGCGAGGTAC; *RUNX2*:

forward GCAGCAGCAGCAGCAGGAG, reverse GCACCGAGCACAGGAAGTTGG; *OCN*: forward GCCAGGCAGGTGCGAAGC, reverse GTCAGCCAACTCGTCACAGTCC; *GAPDH*: forward CAATGACCCCTTCATTGACC, reverse GACAAGCTTCCCGTTCTCAG.

2.5 Measurement of Intracellular Ca^{2+}

Intracellular Ca^{2+} was monitored ratiometrically using Fura-2. After seeding hDFCs onto sterile glass coverslips and allowing 30 min for attachment, cells were loaded with Fura-2/AM (5 µM) for 30 min at room temperature. The coverslip was then positioned in a 1-mL chamber on a Leica inverted microscope (Leica, Wetzlar, Germany). Cells were perfused for 20 min with a physiological salt solution containing (mM) 130 NaCl, 1.8 $CaCl_2$, 5.4 KCl, 1.0 $MgCl_2$, 10 glucose, and 10 HEPES (pH 7.4). Fluorescence was acquired using the TILLvisION 4.0 imaging system (TILL Photonic, Munich, Germany) coupled to a cooled CCD camera. Ca^{2+} signals were calculated as the F340/F380 ratio based on excitation wavelengths of 340 and 380 nm and emission at 510 nm, with analysis using the $\Delta F/F0$ method. To observe the effects of low $[K^+]_e$ on intracellular Ca^{2+} concentrations, the basal external solution was exchanged for a solution containing low $[K^+]_e$, which was obtained by decreasing $[K^+]_e$ levels and replacing them with equimolar $[Na^+]_e$.

2.6 Immunofluorescence Staining

For immunofluorescence analysis, hDFCs cultured on glass coverslips were first fixed using paraformaldehyde (4%, 20 min) and then subjected to permeabilization with 0.25% Triton X-100 (15 min) and quenching with 3% hydrogen peroxide (15 min). Following blocking with 10% goat serum at 37 °C for 30 min, the cells were probed with primary antibodies targeting Vimentin or CK-14 (both diluted 1:400) at 37 °C for 1 h. After washing with PBS, fluorophore-conjugated secondary antibodies (1:200) were added in the dark and incubated at 37 °C for 1 h. Samples were then counterstained with DAPI (1 min) and examined under a fluorescence microscope.

2.7 Western Blotting

Cells were first lysed in RIPA buffer (PC102, Epizyme Biotech, Shanghai, China) to obtain total protein extracts. Protein concentrations were then assessed via BCA assay (P0011, Beyotime, Shanghai, China). After electrophoretic SDS-PAGE (TF107, Epizyme Biotech, Shanghai, China) separation and transfer onto PVDF membranes (WJ002PS, Epizyme Biotech, Shanghai, China), nonspecific protein binding was blocked using the QuickBlock™ Western blocking reagent (Beyotime Institute of Biotechnology, Shanghai, China) at 37 °C for 15 min. Membranes were then subjected to overnight incubation at 4 °C with primary antibodies specific for Kir2.1 (MA567352, Thermo Fisher Scientific, Waltham, MA, USA), Runx2 (ab23981, Abcam, Cambridge, UK), OCN (ab93876, Abcam, Cambridge, UK), and GAPDH (D16H11, Cell Signaling Technology, Danvers, MA, USA), all at a 1:1000 dilution. After overnight incubation, membranes were washed and probed with secondary antibodies (1:1000, Beyotime, China) for 1 h at room temperature. Signals were developed using ECL reagent (345818, Millipore Corporation, Burlington, MA, USA) and analyzed using ImageJ 1.8.0 (version 1.8.0, NIH, Bethesda, MD, USA), normalizing the results to GAPDH.

2.8 Statistical Analysis

Data are presented as the mean ± SEM. Two-group and multi-group comparisons were made using *t*-tests and one-way ANOVAs, respectively, in GraphPad Prism (v 9.0, GraphPad Software, San Diego, CA, USA).

3. Results

3.1 Membrane Hyperpolarization Is Essential for the Osteogenic Differentiation of hDFCs

hDFCs expressed the MSC marker Vimentin, while lacking the epithelial marker CK-14 (Fig. 1A,B), demonstrating their mesenchymal origin and absence of epithelial contamination. Using these cells, we examined whether membrane hyperpolarization is functionally necessary for hDFC osteogenesis by inducing the osteogenic differentiation of these cells in the presence of high concentrations of extracellular K^+ ($[K^+]_e$), which inhibits membrane hyperpolarization [17], or pinacidil, which opens ATP-sensitive K^+ channels to promote membrane hyperpolarization [17]. As shown in Fig. 1, after 14 days of osteogenic induction, control cells exhibited modest mineralization. Compared with these positive control cells, cells exposed to 50 mM $[K^+]_e$ displayed sparse mineral deposits, whereas those treated with 10 µM pinacidil exhibited robust mineralized nodule formation (Fig. 1C). These findings were corroborated by quantitative analysis of Alizarin red staining (Fig. 1D). ALP, OCN, and RUNX2 are markers of osteogenic differentiation, are critical to osteogenesis and matrix mineralization [18]. In these experiments, ALP activity (Fig. 1E,F) as well as *RUNX2* and *OCN* gene and protein levels decreased in cells treated with 50 mM $[K^+]_e$ relative to positive control conditions, whereas they increased with pinacidil treatment (Fig. 2A–J). Taken together, these data suggest that membrane hyperpolarization is essential for the osteogenic differentiation of hDFCs.

3.2 Kir2.1 Controls the Osteogenic Differentiation of hDFCs

Kir2.1 channels are responsible for the hyperpolarized membrane potentials observed in various cell types. To test the effect of Kir2.1 on hDFC differentiation, we first examined Kir2.1 gene and protein expression levels in hDFCs before and after osteogenic differentiation by qRT-PCR and Western blotting. As shown in Fig. 3A–C, Kir2.1 gene and

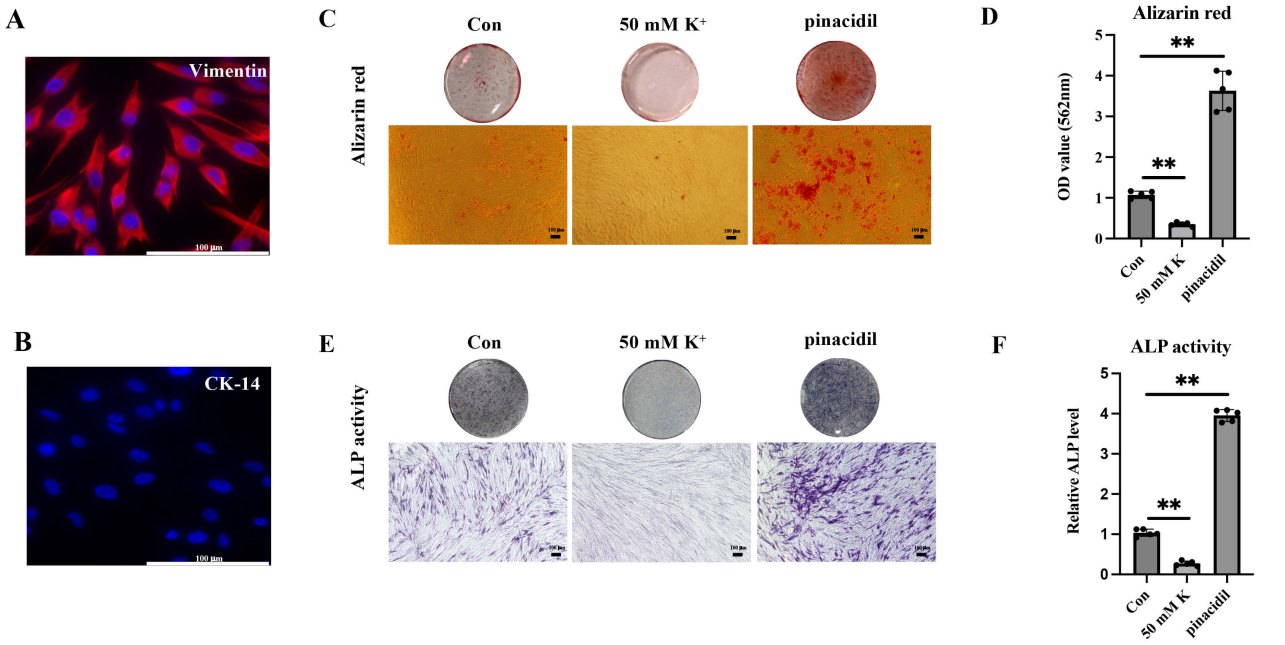


Fig. 1. Membrane potential controls the osteogenic differentiation of hDFCs. Cells were induced in osteogenic medium for 14 days in the absence or presence of 50 mM $[K^+]_e$ or 10 μM pinacidil. (A) Vimentin and DAPI staining. Scale bar: 100 μm. (B) CK-14 and DAPI staining. Scale bar: 100 μm. (C) hDFC mineralization was assessed via Alizarin red staining. (D) Semi-quantitative analysis of Alizarin red staining at 562 nm. (E) ALP staining. (F) ALP activity was detected via colorimetric assay in cell lysates of hDFCs. (C,E) Upper panel: As observed by the naked eye; lower panel: As observed by microscopy (magnification: 200×). Scale bar: 100 μm. Osteogenic media served as a control treatment. Bars represent the mean ± SEM, $^{**}p < 0.01$. hDFCs, human dental follicle stem cells; CK-14, cytokeratin-14; ALP, alkaline phosphatase.

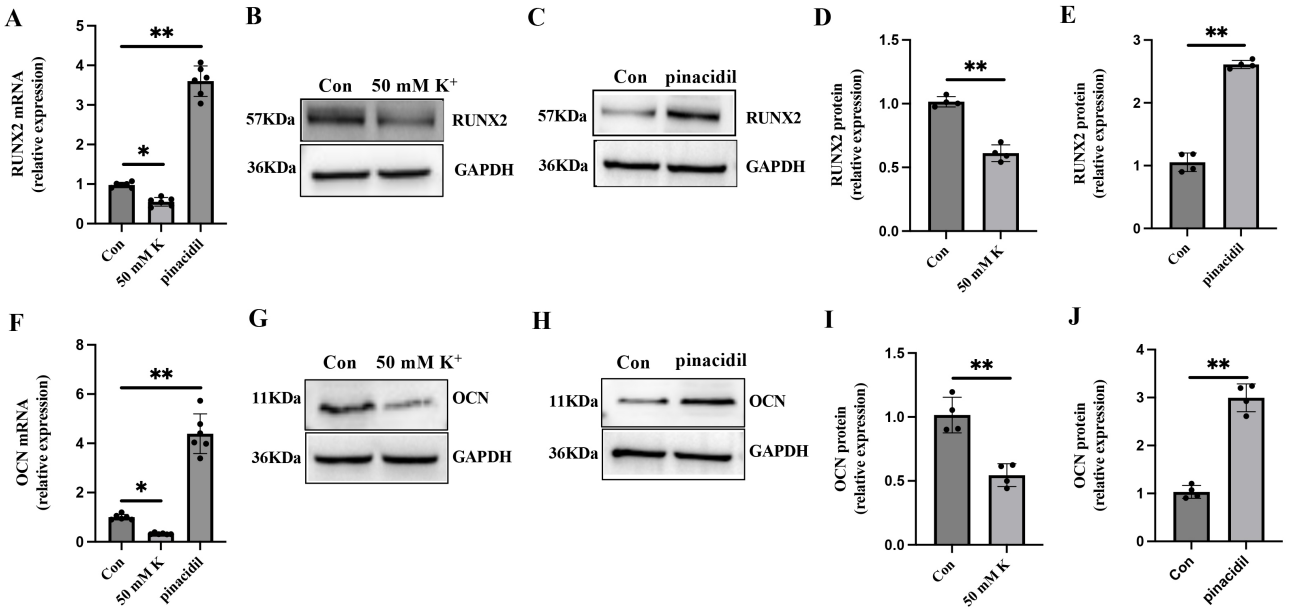


Fig. 2. Membrane potential controls osteogenic marker expression in hDFCs. Cells were induced in osteogenic medium for 14 days in the absence or presence of 50 mM $[K^+]_e$ or 10 μM pinacidil. (A) *RUNX2* gene expression levels were determined by qRT-PCR. (B,C) RUNX2 protein levels were determined by Western blotting. (D,E) Relative band densities in (B,C). (F) *OCN* gene expression levels were determined by qRT-PCR. (G,H) OCN protein levels were determined by Western blotting. (I,J) Relative band densities in (G,H). Osteogenic media served as a control treatment. Bars represent the mean ± SEM, $^{*}p < 0.05$, $^{**}p < 0.01$. RUNX2, runt-related transcription factor 2; qRT-PCR, quantitative real-time polymerase chain reaction; OCN, osteocalcin.

IMR Press

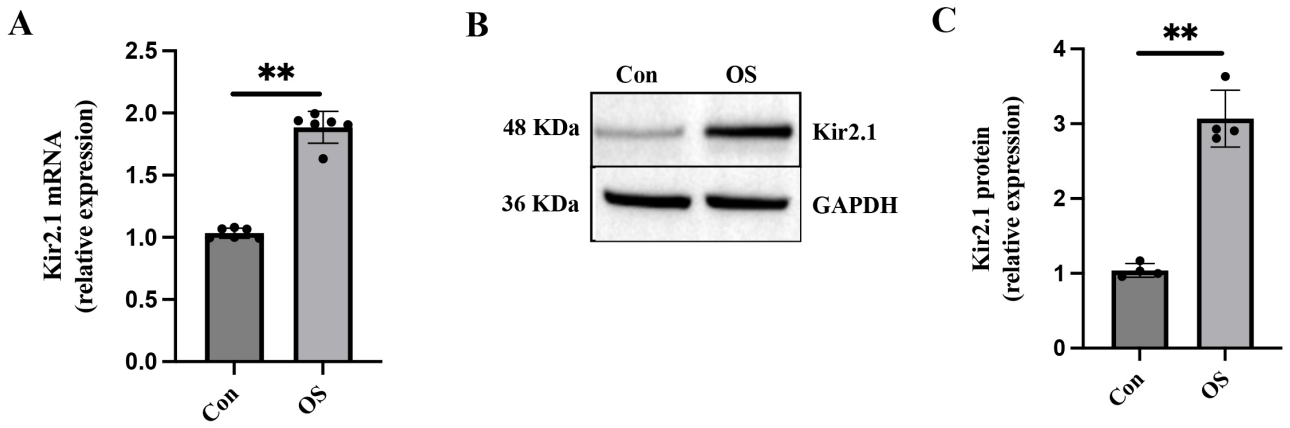


Fig. 3. Kir2.1 is upregulated during the osteogenic differentiation of hDFCs. Cells were induced in osteogenic medium for 14 days. (A) *KCNJ2* mRNA expression levels were determined by qRT-PCR. (B) Kir2.1 protein levels were determined by Western blotting. (C) Relative band density in (B). Basal media served as the control treatment. OS, osteogenic medium; *KCNJ2*, potassium inwardly rectifying channel subfamily J member 2. Bars represent the mean ± SEM, $^{**}p < 0.01$.

protein expression levels increased with osteogenic differentiation.

Next, we explored the potential association between increased Kir2.1 expression levels and the osteogenic differentiation of hDFCs. We generated hDFCs in which Kir2.1 had been stably knocked down, confirming the efficiency of Kir2.1 knockdown by qRT-PCR and Western blotting (Fig. 4A–C). On day 14 of osteogenic differentiation, the osteogenic capacity of the Kir2.1 knockdown cells and that of the cells treated with ML133 (a Kir2.1-specific pharmacological inhibitor) was significantly inhibited compared to the positive control cells, as demonstrated by analyses of mineralization capacity (Fig. 4D,E), ALP activity (Fig. 4F,G). Furthermore, the gene and protein expression of RUNX2 and OCN of the Kir2.1 knockdown cells were significantly decreased compared to the positive control cells (Fig. 5A–F). These results indicated that Kir2.1 regulates the osteogenic differentiation of hDFCs.

3.3 Kir2.1-Linked Membrane Hyperpolarization Increases Intracellular Ca^{2+} Levels in hDFCs

Ca^{2+} plays an essential role in stem cell differentiation, and membrane potential is a key regulator of intracellular Ca^{2+} levels. Therefore, we next performed single-cell Ca^{2+} imaging to determine whether membrane hyperpolarization modulates intracellular Ca^{2+} signaling in hDFCs. As decreasing $[K^+]_e$ is a standard method of hyperpolarizing cells [19], we decreased $[K^+]_e$ to 1 mM and observed the effects of low $[K^+]_e$ on intracellular Ca^{2+} levels in hDFCs. Perfusion with 1 mM $[K^+]_e$ increased intracellular Ca^{2+} levels in hDFCs, as evidenced by a rapid upstroke before reaching a steady state (Fig. 6A). To confirm that Kir2.1-linked membrane hyperpolarization controls the osteogenic differentiation of hDFCs by increasing intracellular Ca^{2+} levels, we observed the effects of low $[K^+]_e$ on intracellular Ca^{2+} levels in Kir2.1 knockdown cells and in cells pretreated with ML133. Kir2.1 knockdown or pretreatment with ML133 significantly suppressed the effects of low $[K^+]_e$ on the intracellular Ca^{2+} levels (Fig. 6B,C,E). The average cell responses are shown in Fig. 6D. These results demonstrate that Kir2.1-linked membrane hyperpolarization increases intracellular Ca^{2+} levels in hDFCs.

3.4 Identification of Ca^{2+} Entry Pathways Responsible for Membrane Hyperpolarization in hDFCs

Next, we sought to determine whether the elevation of intracellular Ca^{2+} levels resulting from membrane hyperpolarization was a result of Ca^{2+} entry across the plasma membrane. To that end, we removed Ca^{2+} from the bath solution and tested the effects of low $[K^+]_e$ on intracellular Ca^{2+} levels in hDFCs. The low $[K^+]_e$-induced increase in intracellular Ca^{2+} levels was abolished by the removal of extracellular Ca^{2+} (Fig. 7A), demonstrating that membrane hyperpolarization caused Ca^{2+} entry across the plasma membrane.

SOCs and L-type voltage-gated Ca^{2+} channels are the most important Ca^{2+}-permeable channels that mediate Ca^{2+} entry in most non-excitable cells. Previous studies have demonstrated that MSCs express both of these channels [13,20,21]. To investigate the Ca^{2+} entry pathways on the hDFC plasma membrane associated with membrane hyperpolarization-induced Ca^{2+} entry, we first tested the effects of nifedipine, an L-type Ca^{2+} channel blocker, on the elevation of intracellular Ca^{2+} induced by membrane hyperpolarization. As shown in Fig. 7B,F, pretreatment with 1 μM nifedipine had no significant effect on the elevation of intracellular Ca^{2+} levels observed in response to low $[K^+]_e$. To test the contribution of SOCs to this effect, we first pretreated hDFCs with 1 μM thapsigargin (TG; a Ca^{2+} pump blocker) in a Ca^{2+}-free solution to deplete the intracellular Ca^{2+} store, followed by perfusion with extracellular solu-

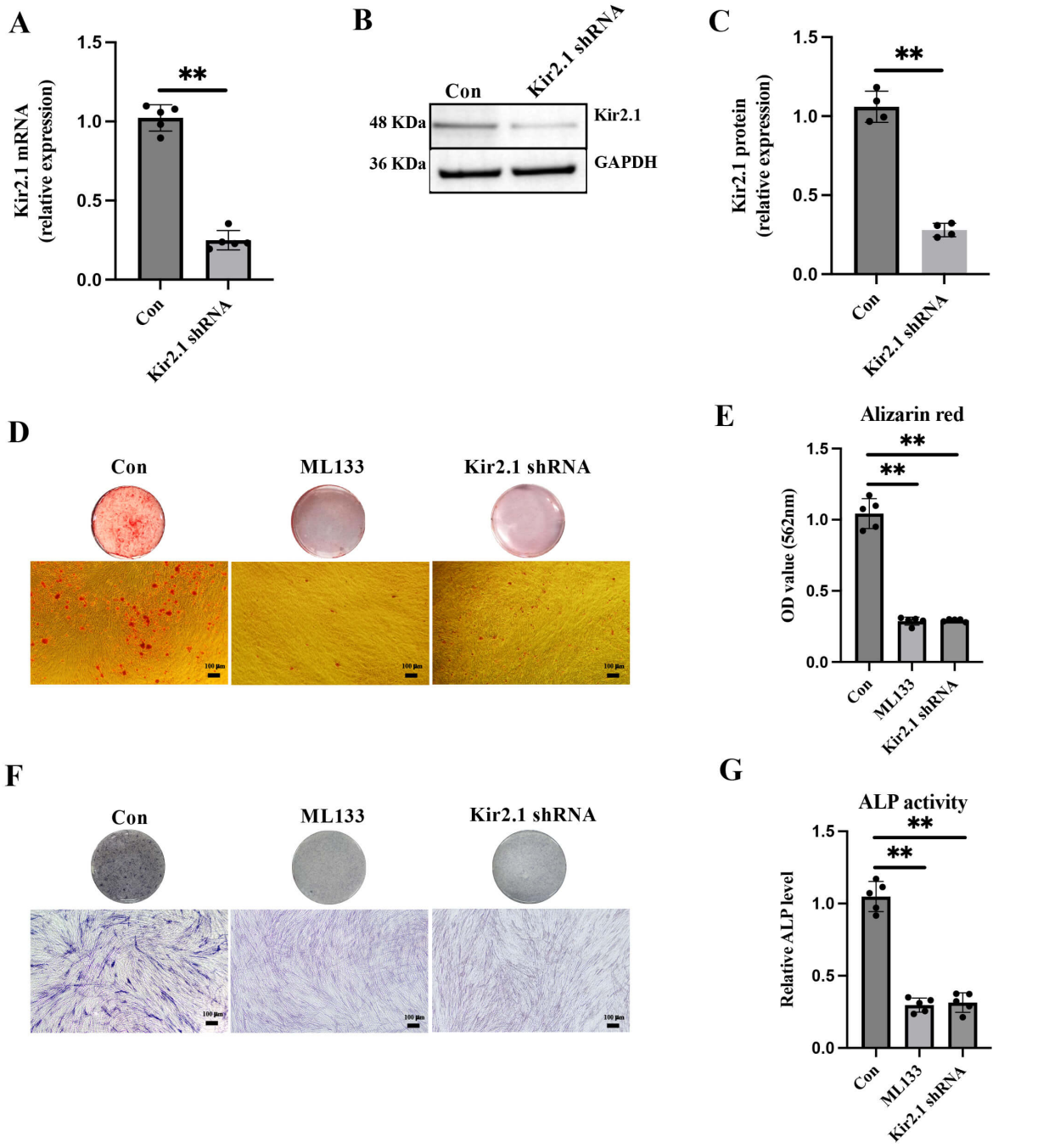


Fig. 4. Inhibition of Kir2.1 suppresses the osteogenic differentiation of hDFCs. (A) Kir2.1 gene expression levels were determined by qRT-PCR. (B) Kir2.1 protein levels were determined by Western blotting. (C) Relative band density in (B). Cells transfected with a scrambled shRNA served as the control group. Cells transfected with a scrambled shRNA or Kir2.1 shRNA were induced in osteogenic medium for 14 days in the absence or presence of 20 μM ML133. (D) Mineralization of hDFCs was assessed via Alizarin red staining. (E) Semi-quantitative analysis of Alizarin red staining at 562 nm. (F) appearance of ALP staining is shown. (G) ALP activity was detected via colorimetric assay in cell lysates of hDFCs. (D,F) Upper panel: As observed by the naked eye; lower panel: as observed by microscopy (magnification: 200×). Scale bar: 100 μm. Cells transfected with scrambled shRNA induced in osteogenic media served as a control group. Bars represent the mean ± SEM, $^{**}p < 0.01$. shRNA, short hairpin RNA.

tions containing 4 mM Ca^{2+}. This experimental design is a classical means of characterizing SOC-mediated Ca^{2+} entry [22]. As shown in Fig. 7C, perfusion with Ca^{2+}-free solutions containing 1 μM TG induced intracellular Ca^{2+} release, and the addition of 4 mM Ca^{2+} caused SOC-mediated Ca^{2+} entry. We then tested the effects of 0.1 mM La^{3+}, a

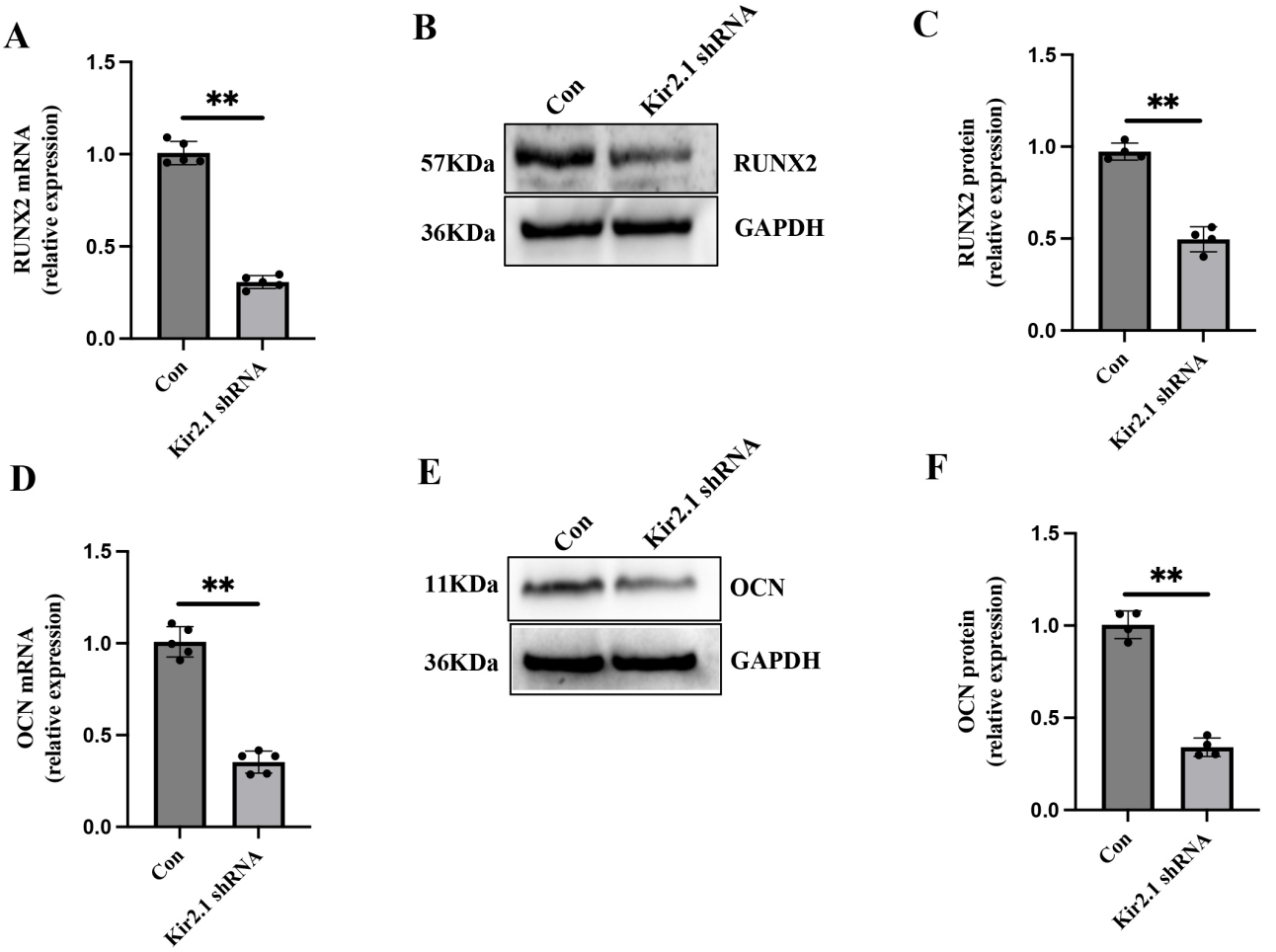


Fig. 5. Inhibition of Kir2.1 attenuates osteogenic marker expression by hDFCs. Cells transfected with a scrambled shRNA or Kir2.1 shRNA were induced in osteogenic medium for 14 days. (A) *RUNX2* gene expression levels were determined via qRT-PCR. (B) RUNX2 protein levels were determined by Western blotting. (C) Relative band density values in (B). (D) *OCN* gene expression levels were determined utilizing qRT-PCR. (E) OCN protein expression levels were determined by Western blotting. (F) Relative band density in (E). Cells transfected with the scrambled shRNA induced in osteogenic media served as a control group. Bars represent the mean ± SEM, $^{**}p < 0.01$.

blocker of SOCs, on the elevation of intracellular Ca^{2+} levels observed in response to membrane hyperpolarization. As shown in Fig. 7D,F, pretreatment with 0.1 mM La^{3+} dramatically inhibited the effects of low $[K^+]_e$ on intracellular Ca^{2+}. Average cellular responses are shown in Fig. 7E,F. These results demonstrate that SOC-mediated Ca^{2+} entry across the plasma membrane contributes to the membrane hyperpolarization-induced elevation of the intracellular Ca^{2+} levels in hDFCs.

4. Discussion

Studies on Andersen's syndrome-induced pluripotent stem cells and *KCNJ2* knockout animal models have revealed the important role of Kir2.1 channels in osteoblastic processes and bone development [8,9,23,24,25]. However, the electrophysiological mechanisms by which Kir2.1 channels control the osteogenic differentiation of MSCs remain poorly understood. In this study, we explored the precise relationship between Kir2.1 channels and the osteogenic differentiation of MSCs in detail. We found that Kir2.1 channel-linked membrane hyperpolarization controls MSC osteogenic differentiation by increasing intracellular Ca^{2+} levels, and we determined that SOC-mediated Ca^{2+} influx is essential for this process.

Using hDFCs, we first demonstrated that membrane hyperpolarization is an essential prerequisite for the induction of osteogenic differentiation activity in hDFCs. We found that the reversal of membrane hyperpolarization achieved by increasing $[K^+]_e$ suppressed hDFC osteogenic differentiation, whereas promoting membrane hyperpolarization by opening ATP-sensitive K^+ channels enhanced the osteogenic differentiation of hDFCs. This finding is consistent with previous results demonstrating that endogenous membrane hyperpolarization is a functional determinant of

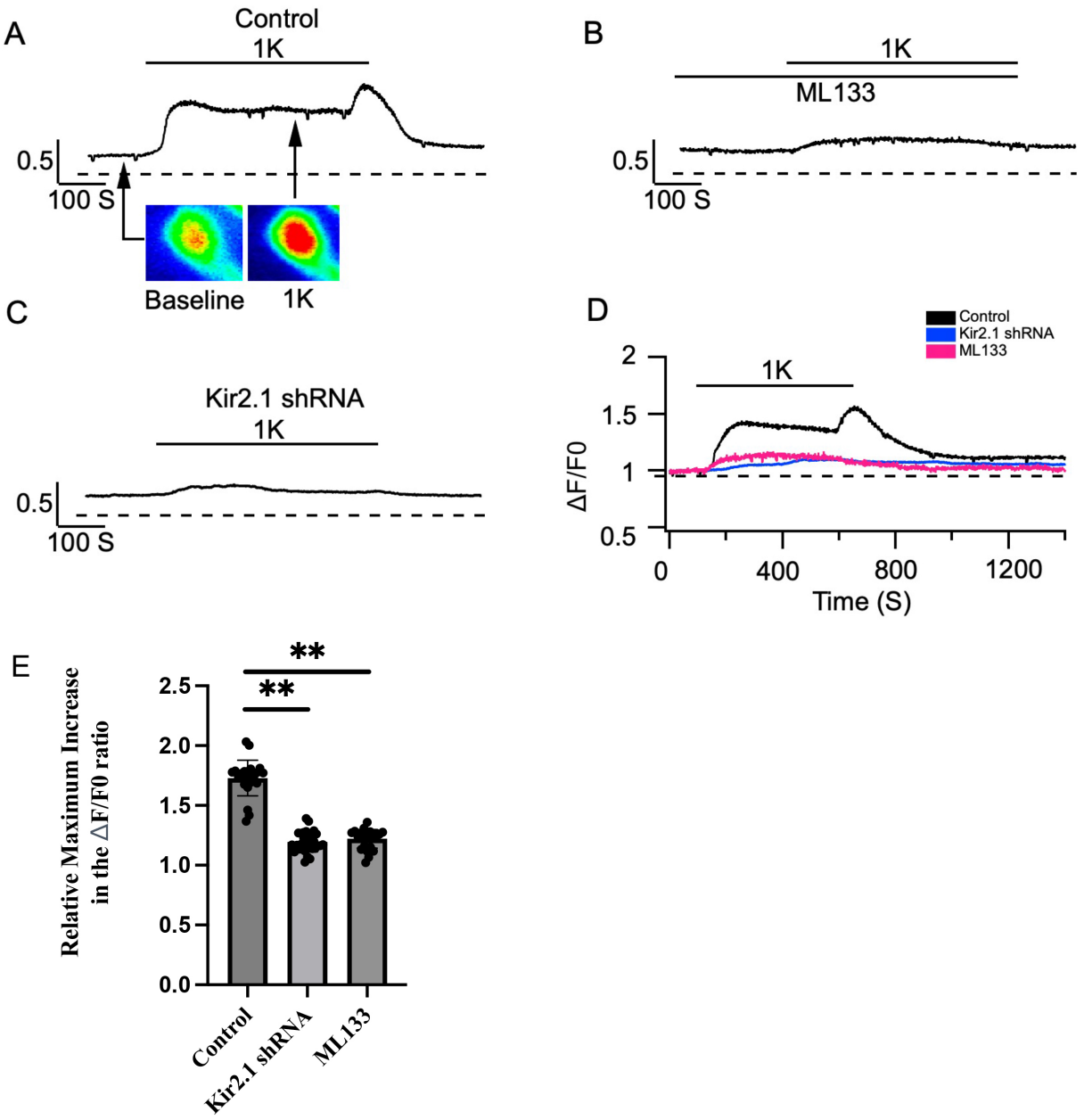


Fig. 6. Kir2.1 contributes to low $[K^+]_e$-induced elevation of intracellular Ca^{2+} levels in hDFCs. (A) Upper panel: Ca^{2+} levels from hDFCs in response to 1 mM $[K^+]_e$. Lower panel: Representative fluorescence images from the indicated time points in the experiments shown in the upper panel. (B) Ca^{2+} levels from hDFCs exposed to 1 mM $[K^+]_e$ in the presence of ML133. (C) Ca^{2+} levels from Kir2.1 knockdown hDFCs exposed to 1 mM $[K^+]_e$. (D) Average Ca^{2+} levels in hDFCs exposed to 1 mM $[K^+]_e$. (E) Relative maximum increase in the ΔF/F0 ratio from indicated groups of hDFCs in response to 1 mM $[K^+]_e$. Control hDFCs (n = 24 cells), Kir2.1 knockdown hDFCs (n = 32 cells), and hDFCs exposed to ML133 (n = 26 cells). The total cells are from 5 independent biological replicates. Bars represent the mean ± SEM, $^{**}p < 0.01$.

MSC osteogenic differentiation [17]. Second, we determined that Kir2.1 channels are responsible for the hyperpolarized membrane-linked osteogenic differentiation of hDFCs. We showed that the gene and protein expression levels of Kir2.1 increased with hDFC osteogenic differentiation, suggesting that Kir2.1 is responsible for hDFCs differentiation. To test this hypothesis, we examined the effects of Kir2.1-specific shRNA or pharmacological inhibitor treatment on hDFCs. This approach revealed that shRNA- or ML133-mediated inhibition of Kir2.1 suppressed hDFC osteogenic differentiation, clearly demonstrating the essential role of Kir2.1 in this process. Similarly, Fischer-Lougheed et al. [26] and Liu et al. [27] reported that Kir2.1-linked membrane hyperpolarization initiates the process of dif-

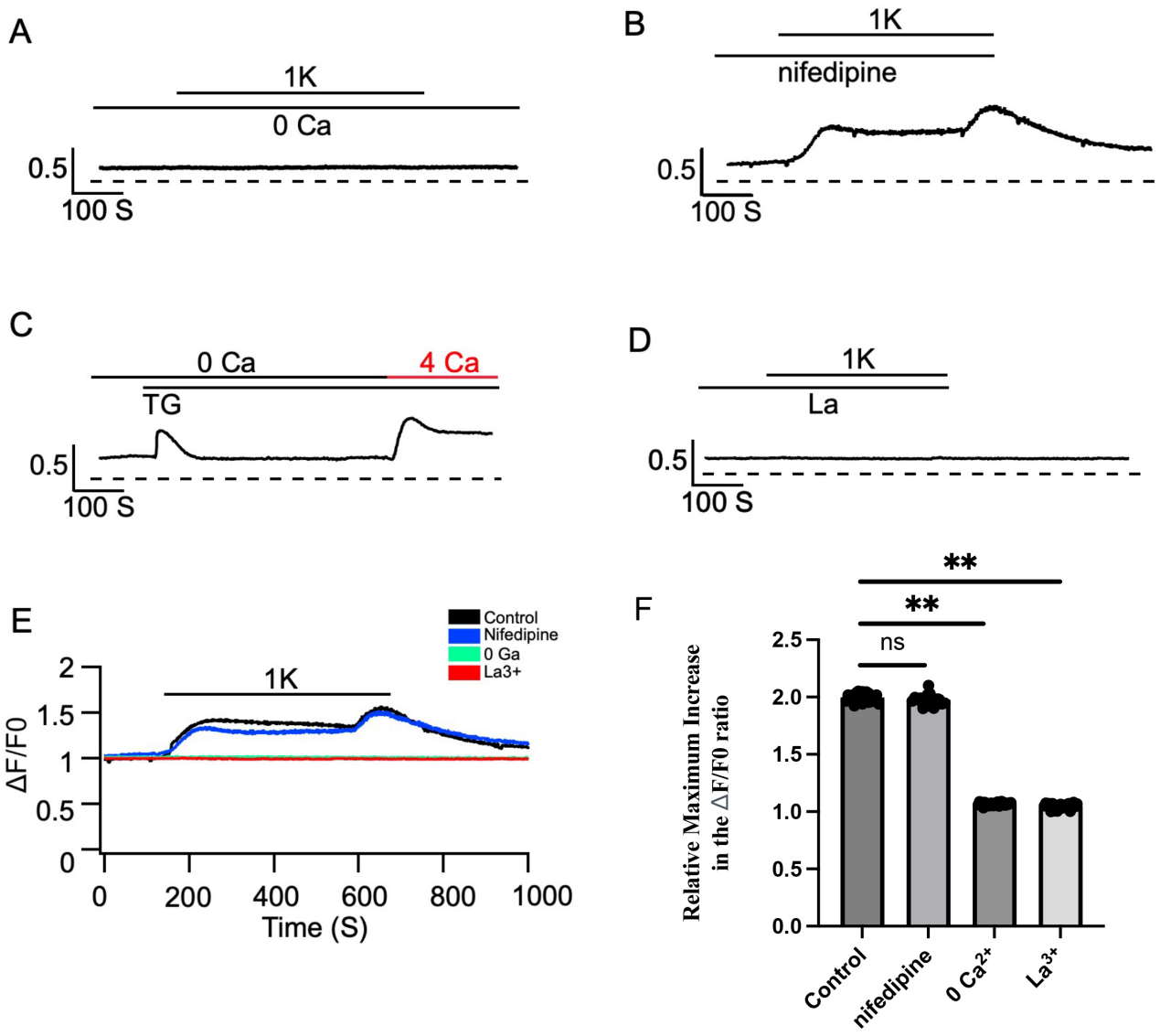


Fig. 7. SOC-mediated Ca^{2+} influx in response to low $[K^+]_e$ in hDFCs. (A) Removal of extracellular Ca^{2+} eliminated the low $[K^+]_e$-induced elevation of intracellular Ca^{2+} levels in hDFCs. (B) Ca^{2+} levels from hDFCs in response to 1 mM $[K^+]_e$ in the presence of nifedipine. (C) TG-induced store-operated Ca^{2+} entry in hDFCs (n = 8 cells). (D) hDFC Ca^{2+} levels in response to 1 mM $[K^+]_e$ in the presence of La^{3+}. (E) Average Ca^{2+} levels in response to 1 mM $[K^+]_e$. (F) Relative maximum increase in the ΔF/F0 ratio from indicated groups of hDFCs in response to 1 mM $[K^+]_e$. Control hDFCs (n = 24 cells), hDFCs in the presence of nifedipine (n = 18 cells) or La^{3+} (n = 21 cells), or in the absence of extracellular Ca^{2+} (n = 26 cells). Bars represent the mean ± SEM, ns, not statistically significant. $^{**}p < 0.01$. SOC, store-operated Ca^{2+} channel.

ferentiation by maintaining membrane hyperpolarization in human myoblasts. Moreover, Komarova et al. [28] and Weidema et al. [29] reported that Kir2.1 participates in the regulation of osteoclast physiological function by maintaining membrane hyperpolarization. As multiple K^+ channel subtypes are expressed in MSCs and hDFCs are dental-derived MSCs, we cannot exclude the effects of other K^+ channel subtypes when considering these results. However, in light of the results from gene knockdown and pharmacological inhibition experiments, we conclude that Kir2.1 acts as the key regulator of osteogenic differentiation, although future studies focused on the potential contributions of other K^+ channels may be warranted.

An increase in intracellular Ca^{2+} levels is frequently observed during stem cell differentiation [30]. To investigate the mechanisms by which membrane hyperpolarization regulates the osteogenic differentiation of hDFCs, we performed single-cell Ca^{2+} imaging to observe the effects of low $[K^+]_e$ on the intracellular Ca^{2+} levels in these cells. We found that low $[K^+]_e$-induced membrane hyperpolarization triggered an increase in intracellular Ca^{2+} levels in hDFCs, and this phenomenon was significantly suppressed

by Kir2.1 knockdown or treatment with ML133. These results demonstrate that Kir2.1-linked membrane hyperpolarization increased intracellular Ca^{2+} levels in hDFCs. In line with this finding, Kir2.1-dependent membrane hyperpolarization has been shown to raise cytosolic Ca^{2+} levels, which are indispensable for proper myoblast differentiation [31].

We additionally investigated the Ca^{2+} entry pathways responsible for membrane hyperpolarization-induced increases in intracellular Ca^{2+} levels in hDFCs. Through this approach, we determined that the low $[K^+]_e$-induced increase in intracellular Ca^{2+} levels was abolished by the removal of extracellular Ca^{2+}, demonstrating that membrane hyperpolarization induces Ca^{2+} entry across the plasma membrane in hDFCs. We next investigated the role of L-type Ca^{2+} channels in this process, revealing that membrane hyperpolarization-induced increases in intracellular Ca^{2+} levels were unaffected when these L-type Ca^{2+} channels were blocked. This supports previous findings that L-type Ca^{2+} channel function is dispensable for the osteogenic differentiation of hMSCs [32]. SOCs are considered the main Ca^{2+} entry pathways at the plasma membrane of non-excitable cells, such as DFCs of mesenchymal origin [33]. We also confirmed the existence of SOC-mediated Ca^{2+} entry in hDFCs and further demonstrated that the membrane hyperpolarization-induced increase in intracellular Ca^{2+} levels was abolished by blocking SOCs. Membrane depolarization has been reported to convert physiological Ca^{2+} oscillations into sustained Ca^{2+} elevations in T lymphocytes as a result of the disruption of the driving force for Ca^{2+} entry through SOCs [34]. Our results concur with previous reports that Ca^{2+} entry through the plasma membrane is primarily mediated by SOCs, with a more limited contribution from voltage-gated Ca^{2+} channels in MSCs [11,32].

Limitations

This study has several inherent limitations. First, membrane potential was modulated indirectly via extracellular K^+ manipulation and pharmacological treatments, whereas direct measurement using voltage-sensitive dyes was not performed. In addition, Kir2.1 expression was only examined at day 14 of osteogenic induction, without any detailed time-course analysis aimed at defining its stage-specific expression characteristics. However, our results support a temporal correlation, as the shRNA- or ML133-mediated inhibition of Kir2.1 significantly suppressed early markers of osteogenesis (ALP activity and Runx2 expression) and abolished the hyperpolarization-induced Ca^{2+} response, indicating that Kir2.1 activity is required before initiating the matrix maturation and mineralization phases. Pini et al. [8] demonstrated that Kir2.1 is critical for early osteogenic and chondrogenic commitment, functioning upstream of master transcription factors such as Runx2. Our findings align with previous reports that Kir2.1 plays a central role during the early stages of differentiation to enable master osteogenic gene expression. While we confirmed the dominant role of Kir2.1 in osteogenic differentiation, the potential contributions of other endogenous K^+ channels in hDFCs were not fully evaluated. Though we verified that SOC channels mediate Ca^{2+} influx upon membrane hyperpolarization, the detailed regulatory network that defines this signaling cascade requires further investigation.

5. Conclusions

This study describes, for the first time, the electrophysiological mechanisms by which Kir2.1 regulates MSC osteogenesis. Using hDFCs, we demonstrated that Kir2.1-linked membrane hyperpolarization controls the osteogenic differentiation of these cells by mediating Ca^{2+} entry across the plasma membrane and that SOCs play an important role in this process. This study extends the findings of previous research focused on the relationship between membrane potential and MSC differentiation, highlighting a novel electrophysiological mechanism that controls osteogenic differentiation of MSCs.

Availability of Data and Materials

The datasets used and analyzed during the current study are available from the corresponding author on reasonable request.

Author Contributions

YY, WD, DY, YL, and DZ conducted experiments. JZ designed the research study, performed the research, wrote the manuscript, and analyzed the data. All authors contributed to editorial changes in the manuscript. All authors read and approved the final manuscript. All authors have participated sufficiently in the work and agreed to be accountable for all aspects of the work.

Ethics Approval and Consent to Participate

Dental follicles were obtained from embedded third molars collected from the orthodontics department at the Affiliated Stomatology Hospital of Southwest Medical University in Luzhou, China. Ethical approval for all human cell culture experiments was obtained from the Ethics Committee of the Affiliated Stomatology Hospital of Southwest Medical University (reference number: 220815003). Informed consent was obtained from the patient or guardian. The study was carried out in accordance with the guidelines of the Declaration of Helsinki.

Acknowledgment

We would like to express our gratitude to all those who helped us during the writing of this manuscript and thank to all the peer reviewers for their opinions and suggestions.

Funding

This work was supported by Sichuan Science and Technology Program (2024NSFSC2103 and 2023NS-

FSC1522); Southwest Medical University Stomatology Special Program (2024KQZX10); The Supervisory Team Capacity Building Grant Project from the Affiliated Stomatology Hospital of Southwest Medical University (2025DS01).

Conflicts of Interest

The authors declare no conflicts of interest.

References

[1] Morsczeck C, Reichert TE. Dental stem cells in tooth regeneration and repair in the future. Expert Opinion on Biological Therapy. 2018; 18: 187–196. https://doi.org/10.1080/14712598.2018.1402004

[2] Zhou T, Pan J, Wu P, Huang R, Du W, Zhou Y, et al. Dental Follicle Cells: Roles in Development and Beyond. Stem Cells International. 2019; 2019: 9159605. https://doi.org/10.1155/2019/9159605

[3] Hibino H, Inanobe A, Furutani K, Murakami S, Findlay I, Kurachi Y. Inwardly rectifying potassium channels: their structure, function, and physiological roles. Physiological Reviews. 2010; 90: 291–366. https://doi.org/10.1152/physrev.00021.2009

[4] Yu W, Wang Z, Yu X, Zhao Y, Xie Z, Zhang K, et al. Kir2.1-mediated membrane potential promotes nutrient acquisition and inflammation through regulation of nutrient transporters. Nature Communications. 2022; 13: 3544. https://doi.org/10.1038/s41467-022-31149-y

[5] Zhang X, Cui X, Li X, Yan H, Li H, Guan X, et al. Inhibition of Kir2.1 channel-induced depolarization promotes cell biological activity and differentiation by modulating autophagy in late endothelial progenitor cells. Journal of Molecular and Cellular Cardiology. 2019; 127: 57–66. https://doi.org/10.1016/j.yjmcc.2018.11.005

[6] Nguyen HL, Pieper GH, Wilders R. Andersen-Tawil syndrome: clinical and molecular aspects. International Journal of Cardiology. 2013; 170: 1–16. https://doi.org/10.1016/j.ijcard.2013.10.010

[7] Simkin D, Robin G, Giuliano S, Vukolic A, Moceri P, Guy N, et al. Andersen's syndrome mutants produce a knockdown of inwardly rectifying K^+ channel in mouse skeletal muscle in vivo. Cell and Tissue Research. 2018; 371: 309–323. https://doi.org/10.1007/s00441-017-2696-7

[8] Pini J, Giuliano S, Matonti J, Gannoun L, Simkin D, Rouleau M, et al. Osteogenic and Chondrogenic Master Genes Expression Is Dependent on the Kir2.1 Potassium Channel Through the Bone Morphogenetic Protein Pathway. Journal of Bone and Mineral Research: the Official Journal of the American Society for Bone and Mineral Research. 2018; 33: 1826–1841. https://doi.org/10.1002/jbmr.3474

[9] Sacco S, Giuliano S, Sacconi S, Desnuelle C, Barhanin J, Amri EZ, et al. The inward rectifier potassium channel Kir2.1 is required for osteoblastogenesis. Human Molecular Genetics. 2015; 24: 471–479. https://doi.org/10.1093/hmg/ddu462

[10] Kawano S, Otsu K, Kuruma A, Shoji S, Yanagida E, Muto Y, et al. ATP autocrine/paracrine signaling induces calcium oscillations and NFAT activation in human mesenchymal stem cells. Cell Calcium. 2006; 39: 313–324. https://doi.org/10.1016/j.ceca.2005.11.008

[11] Kawano S, Shoji S, Ichinose S, Yamagata K, Tagami M, Hiraoka M. Characterization of Ca(2+) signaling pathways in human mesenchymal stem cells. Cell Calcium. 2002; 32: 165–174. https://doi.org/10.1016/s0143416002001240

[12] Sun S, Liu Y, Lipsky S, Cho M. Physical manipulation of calcium oscillations facilitates osteodifferentiation of human mesenchymal stem cells. FASEB Journal: Official Publication of the Federation of American Societies for Experimental Biology. 2007; 21: 1472–1480. https://doi.org/10.1096/fj.06-7153com

[13] Jiang LH, Mousawi F, Yang X, Roger S. ATP-induced Ca^{2+}-signalling mechanisms in the regulation of mesenchymal stem cell migration. Cellular and Molecular Life Sciences: CMLS. 2017; 74: 3697–3710. https://doi.org/10.1007/s00018-017-2545-6

[14] Behringer EJ, Segal SS. Membrane potential governs calcium influx into microvascular endothelium: integral role for muscarinic receptor activation. The Journal of Physiology. 2015; 593: 4531–4548. https://doi.org/10.1113/JP271102

[15] Clapham DE. Calcium signaling. Cell. 2007; 131: 1047–1058. https://doi.org/10.1016/j.cell.2007.11.028

[16] Zuo D, Li J, Huang Y, Li J, Yao S, Xiong L, et al. TRPM7 is Involved in the Regulation of Proliferation, Migration and Osteogenic Differentiation of Human Dental Follicle Cells. Frontiers in Bioscience (Landmark Edition). 2023; 28: 104. https://doi.org/10.31083/j.fbl2805104

[17] Sundelacruz S, Levin M, Kaplan DL. Membrane potential controls adipogenic and osteogenic differentiation of mesenchymal stem cells. PloS One. 2008; 3: e3737. https://doi.org/10.1371/journal.pone.0003737

[18] Ching HS, Luddin N, Rahman IA, Ponnuraj KT. Expression of Odontogenic and Osteogenic Markers in DPSCs and SHED: A Review. Current Stem Cell Research & Therapy. 2017; 12: 71–79. https://doi.org/10.2174/1574888x11666160815095733

[19] Zuo D, Chen K, Zhou M, Liu Z, Chen H. Kir2.1 and K2P1 channels reconstitute two levels of resting membrane potential in cardiomyocytes. The Journal of Physiology. 2017; 595: 5129–5142. https://doi.org/10.1113/JP274268

[20] Heubach JF, Graf EM, Leutheuser J, Bock M, Balana B, Zahanich I, et al. Electrophysiological properties of human mesenchymal stem cells. The Journal of Physiology. 2004; 554: 659–672. https://doi.org/10.1113/jphysiol.2003.055806

[21] Li GR, Sun H, Deng X, Lau CP. Characterization of ionic currents in human mesenchymal stem cells from bone marrow. Stem Cells (Dayton, Ohio). 2005; 23: 371–382. https://doi.org/10.1634/stemcells.2004-0213

[22] Parekh AB, Penner R. Store depletion and calcium influx. Physiological Reviews. 1997; 77: 901–930. https://doi.org/10.1152/physrev.1997.77.4.901

[23] Belus MT, Rogers MA, Elzubeir A, Josey M, Rose S, Andreeva V, et al. Kir2.1 is important for efficient BMP signaling in mammalian face development. Developmental Biology. 2018; 444: S297–S307. https://doi.org/10.1016/j.ydbio.2018.02.012

[24] Dahal GR, Pradhan SJ, Bates EA. Inwardly rectifying potassium channels influence *Drosophila* wing morphogenesis by regulating Dpp release. Development (Cambridge, England). 2017; 144: 2771–2783. https://doi.org/10.1242/dev.146647

[25] Dahal GR, Rawson J, Gassaway B, Kwok B, Tong Y, Ptácek LJ, et al. An inwardly rectifying K+ channel is required for patterning. Development (Cambridge, England). 2012; 139: 3653–3664. https://doi.org/10.1242/dev.078592

[26] Fischer-Lougheed J, Liu JH, Espinos E, Mordasini D, Bader CR, Belin D, et al. Human myoblast fusion requires expression of functional inward rectifier Kir2.1 channels. The Journal of Cell Biology. 2001; 153: 677–686. https://doi.org/10.1083/jcb.153.4.677

[27] Liu JH, Bijlenga P, Fischer-Lougheed J, Occhiodoro T, Kaelin A, Bader CR, et al. Role of an inward rectifier K+ current and of hyperpolarization in human myoblast fusion. The Journal of Physiology. 1998; 510: 467–476. https://doi.org/10.1111/j.1469-7793.1998.467bk.x

[28] Komarova SV, Dixon SJ, Sims SM. Osteoclast ion channels: potential targets for antiresorptive drugs. Current Phar-

maceutical Design. 2001; 7: 637–654. https://doi.org/10.2174/1381612013397799

[29] Weidema AF, Dixon SJ, Sims SM. Electrophysiological characterization of ion channels in osteoclasts isolated from human deciduous teeth. Bone. 2000; 27: 5–11. https://doi.org/10.1016/s8756-3282(00)00287-8

[30] Tonelli FMP, Santos AK, Gomes DA, da Silva SL, Gomes KN, Ladeira LO, et al. Stem cells and calcium signaling. Advances in Experimental Medicine and Biology. 2012; 740: 891–916. https://doi.org/10.1007/978-94-007-2888-2_40

[31] Bijlenga P, Liu JH, Espinos E, Haenggeli CA, Fischer-Lougheed J, Bader CR, et al. T-type alpha 1H Ca2+ channels are involved in Ca2+ signaling during terminal differentiation (fusion) of human myoblasts. Proceedings of the National Academy of Sciences of the United States of America. 2000; 97: 7627–7632. https://doi.org/10.1073/pnas.97.13.7627

[32] Zahanich I, Graf EM, Heubach JF, Hempel U, Boxberger S, Ravens U. Molecular and functional expression of voltage-operated calcium channels during osteogenic differentiation of human mesenchymal stem cells. Journal of Bone and Mineral Research: the Official Journal of the American Society for Bone and Mineral Research. 2005; 20: 1637–1646. https://doi.org/10.1359/JBMR.050521

[33] Nelson P, Ngoc Tran TD, Zhang H, Zolochevska O, Figueiredo M, Feng JM, et al. Transient receptor potential melastatin 4 channel controls calcium signals and dental follicle stem cell differentiation. Stem Cells (Dayton, Ohio). 2013; 31: 167–177. https://doi.org/10.1002/stem.1264

[34] Launay P, Cheng H, Srivatsan S, Penner R, Fleig A, Kinet JP. TRPM4 regulates calcium oscillations after T cell activation. Science (New York, N.Y.). 2004; 306: 1374–1377. https://doi.org/10.1126/science.1098845